

Original Research Article

Synthesis, Crystal Structure, Density Function Theory, Molecular Docking and Antimicrobial Studies of 2-(3-(4-phenylpiperazin-1-yl) propyl) isoindoline-1,3-dione

Hazem A Ghabbour^{1,2*} and Maha M Qabeel³

¹Department of Pharmaceutical Chemistry, College of Pharmacy, King Saud University, Riyadh 11451, Saudi Arabia,

²Department of Medicinal Chemistry, Faculty of Pharmacy, Mansoura University, Mansoura 35516, Egypt, ³Department of Clinical Microbiology and Immunology, College of Medicine, Mansoura University, Mansoura 35516, Egypt

*For correspondence: **Email:** ghabbourh@yahoo.com; **Tel:** +966 146 95853; **Fax:** +966 14676220

Received: 3 September 2015

Revised accepted: 5 January 2016

Abstract

Purpose: To determine the exact structure and antimicrobial activity of 2-(3-(4-phenylpiperazin-1-yl) propyl) isoindoline-1,3-dione.

Methods: 2-(3-(4-Phenylpiperazin-1-yl) propyl) isoindoline-1,3-dione (C₂₁H₂₃N₃O₂) was synthesized by the reaction of phthalimide with 1,3-dibromopropane to form 2-(3-bromopropyl) isoindoline-1,3-dione, and was then treated with 1-phenylpiperazine in acetonitrile. The structure of the title compound, 2-(3-(4-phenylpiperazin-1-yl)propyl)isoindoline-1,3-dione, was characterized by proton nuclear magnetic resonance spectroscopy (NMR) and single crystal x-ray diffraction method. The target compound was tested for its antimicrobial activities and computational studies including density function test (DFT) and docking studies were performed.

Results: The crystal structure is monoclinic, P21/n, a = 10.0047 (3) Å, b = 6.0157 (2) Å, c = 30.8571 (12) Å, β = 90.105 (1) °, V = 1857.14 (11) Å³, Z = 4, wR_{ref}(F²) = 0.158, T = 296 K. The molecules are packed in the crystal structure by non-classical intermolecular C-H...O interactions. Besides HOMO-LUMO energy gap was performed at B3LYP/6-31G (d,p) level of theory. The compound exhibited good activity against *S. aureus* and *C. albicans* with zones of inhibition of 15 cm and 18 cm, respectively

Conclusion: The test compound has a moderate antimicrobial activity and the optimized molecular structure of the studied compound using B3LYP/6-31G (d,p) method showed good agreement with the reported x-ray structure.

Keywords: Isoindoline-1, 3-dione, X-ray analysis, Density function theory, Antimicrobial, Molecular docking

Tropical Journal of Pharmaceutical Research is indexed by Science Citation Index (SciSearch), Scopus, International Pharmaceutical Abstract, Chemical Abstracts, Embase, Index Copernicus, EBSCO, African Index Medicus, JournalSeek, Journal Citation Reports/Science Edition, Directory of Open Access Journals (DOAJ), African Journal Online, Bioline International, Open-J-Gate and Pharmacy Abstracts

INTRODUCTION

Phthalimide (1,3 isoindolinedione) derivatives have been broadly utilized in medicinal chemistry and drug design because of extensive variety of biological activities such as antimicrobial, anti-convulsant, anticancer, anti-inflammatory, analgesic, hypolipidemic and immunomodulatory activities [1]. The use of phthalimide as primary

amine protecting group is extensively reported in the chemical literature, especially in alpha amino acid [2]. On the other hand, N-phenylpiperazine subunit represents one of the most varied scaffolds used in the medicinal chemistry fields [3]. The hybridization between the two groups makes very good chance for many biological activities like human adenosine A2A receptor agonists [4], selective dopamine D3 and D4

agonists [5], selective 5-HT_{2A} receptor antagonists [6] and calcium channel blockers [7].

EXPERIMENTAL

Materials and instrument

All organic solvents and used were obtained from commercial sources and used with further purification. Melting points (°C) were measured in open glass capillaries using Branstead 9001 electrothermal melting point apparatus. ¹H (500 MHz) NMR spectra were obtained on Bruker AC 500 Ultra Shield spectrometer (Fällanden, Switzerland). (ESI-MS) was determined using Agilent Ion Trap Mass Spectrometer. X-ray data collection was carried out on Bruker SMART APEX II CCD diffractometer, cell refinement: SAINT [8]; data reduction: SAINT; program used to solve structure: SHELXS; program used to refine structure: SHELXL; molecular graphics: SHELXTL [9]; software used to prepare material for publication: SHELXTL, PLATON [10] and Mercury [11].

Synthesis of the compounds

The 2-(3-(4-phenylpiperazin-1-yl) propyl) isoindoline-1,3-dione was synthesized by the reaction of phthalimide with 1,3-dibromopropane to give 2-(3-bromopropyl)isoindoline-1,3-dione which in turn reacted with N-phenylpiperzine and potassium carbonate in acetonitrile (Scheme 1).

2-(3-Bromopropyl) isoindoline-1,3-dione (**2**): 3.20 g (22 mmol) of phthalimide (**1**) was added to 4.40 g (22 mmol) of 1,3-dibromopropane and 6.08 g (44 mmol) of potassium carbonate in 100 mL of DMF. The mixture was stirred at RT for 3 h and then poured into ice. The resulting mixture was filtered and then crystallized from ethanol. Yield 80 %, Melting Point 72-74 °C [12]

2-(3-(4-Phenylpiperazin-1-yl)propyl)isoindoline-1,3-dione (**3**): 3.00 g (19 mmol) of 1-phenylpiperazine was added to 4.90 g (19 mmol) of 2-(3-bromopropyl)isoindoline-1,3-dione and 6.08 g (44 mmol) of potassium carbonate in 100 mL of acetonitrile. The mixture was allowed to reflux for 3 h. On cooling the acetonitrile was evaporated off and the residue extracted with 150 mL water and 150 mL ethylacetate. The aqueous layer was extracted with 2 × 100 mL

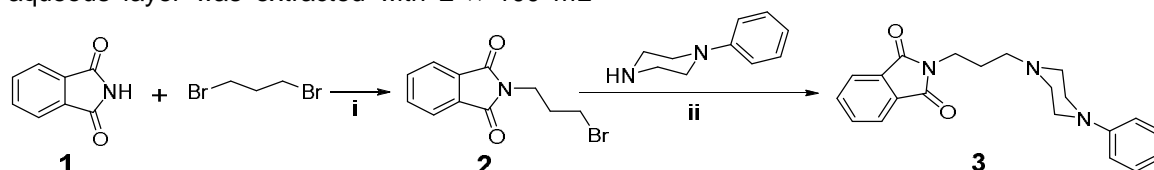
ethyl acetate and combined to the organic layer. The solvent was evaporated off to give a pale yellow product. The product was recrystallized from hexane as pale yellow crystals, 4.2 g (12.03 mmol). Yield 65 %, Melting Point 135-137 °C. ¹H NMR δ (ppm) (CDCl₃): 7.87-7.68 (m, 4 H), 7.45-6.81 (m, 5 H), 3.80 (2 H, t, J = 6.90 Hz), 3.13-3.08 (2 H, m), 2.55-2.44 (8 H, m), 1.88 (q, 2 H). MS (ESI) (*m/z*): [M+H]⁺ 350.28.

Crystal data and structure determination

A yellow plate single crystal with approximate dimension of 0.37 mm × 0.25 mm × 0.24 mm was mounted on a glass fiber in a random orientation. The data were collected by Bruker APEX-II D8 Venture diffractometer with graphite monochromated Mo K α radiation ($\lambda = 0.071073$ nm) using ϕ and ω scans mode in the range of $2.6^\circ \leq \theta \leq 30.6^\circ$ at 293(2) K. A total of 70846 reflections were collected with 5701 unique ones ($R_{int} = 0.055$), of which 3507 reflections with $[I > 2\sigma(I)]$ were considered to be observed and used in the succeeding refinements. The structure was solved by direct methods and expanded by using Fourier differential techniques with SHELXS-97. All non-hydrogen atoms were located with successive difference Fourier syntheses. The structure was refined by full-matrix least-squares method on F² with anisotropic thermal parameters for all non-hydrogen atoms. Full matrix least-squares refinement gave the final $R = 0.055$ and $wR = 0.158$. Crystal data and structure refinement for the title compound are shown in Table 1.

Computational studies

All the quantum chemical calculations in this study were done by applying DFT method with a hybrid functional B3LYP [13] at 6-31G (d,p) double-zeta basis set with polarization functions on heavy and hydrogen atoms [14] using Gaussian 09 software [15]. The geometry was optimized by energy minimization with respect to all the geometrical parameters without considering any molecular symmetry constraints. Drawing the structure of the optimized geometry and visualization of the HOMO and LUMO calculations have been done by GaussView5.0.8 program [16].



Scheme 1: Reagents and conditions: (i) K₂CO₃, DMF, RT, 3 h, (ii) K₂CO₃, acetonitrile, reflux, 3 h

Table 1: Crystal data and structure refinement for compound **3**

Chemical formula	C ₂₁ H ₂₃ N ₃ O ₂
M_r	349.42
Crystal system, space group	Monoclinic, P2 _{1/n}
Temperature (K)	296
a, b, c (Å)	10.0047 (3), 6.0157 (2), 30.8571 (12)
β (°)	90.105 (1)
V (Å³)	1857.14 (11)
Z	4
Radiation type	Mo Kα
μ (mm⁻¹)	0.08
Crystal size (mm)	0.37 × 0.25 × 0.24
Data collection	
Diffractometer	Bruker APEX-II D8 Venture diffractometer
Absorption correction	Multi-scan, SADABS V2012/1 (Bruker AXS Inc.)
T_{min}, T_{max}	0.92, 0.98
No. of measured, independent and observed [I > 2σ(I)] reflections	70846, 5701, 3507
R_{int}	0.055
Refinement	
R[F² > 2σ(F²)], wR(F²), S	0.055, 0.158, 1.00
No. of reflections	5701
No. of parameters	235
H-atom treatment	H-atom parameters constrained
Δρ_{max}, Δρ_{min} (e Å⁻³)	0.24, -0.16

Evaluation of antimicrobial activity

Antimicrobial activities of the compound **3** were determined by using agar well diffusion method [17]. This was used to examine the susceptibility of the reference microorganisms to the tested compound. Two types of petri dishes were prepared; one with a base layer of Mueller-Hinton agar medium (MHA, Becton Dickinson) and the other with Sabouraud agar. The reference microorganism colonies were suspended in 0.85 % saline solution and the turbidity compared with the 0.5 McFarland standards, to produce a suspension of 1.5×10^8 CFU/mL. Subsequently, equidistant (0.6 cm diameter) holes were made using sterile cork borer in the agar. 100 μL of the tested compound solution at concentration (100 μmol dissolved in 1mL DMSO) was poured in the holes. Ciprofloxacin (50 μg/mL) was used as standard for antibacterial and fluconazole (25 μg/mL) was used as standard for antifungal activity, as positive controls. DMSO solvent was used as negative control. The prepared plates were incubated at 37 °C for 24 h and 48 h for bacterial strains and yeast, respectively. The antibacterial activity of the standard drugs and tested compound was expressed as the mean of inhibition diameters produced in mm. In this study, five reference strains were used: *Escherichia coli* ATCC 10536, *Pseudomonas aeruginosa* ATCC 15442, *Staphylococcus aureus* ATCC 6538, *Klebsiella pneumoniae* ATCC 13883 and *Candida albicans* ATCC 90029.

Molecular docking studies

Docking studies was performed for the tested compound in order to understand the mechanism of action as anti-microbial and anti-fungal, molecular modelling and docking studies were performed on X-ray crystal structure of *E. coli* 24kda domain in complex with clorobiocin (PDB code: 1KZN) [18] and cytochrome P450 14α-sterol demethylase from *Mycobacterium tuberculosis* (*Mycobacterium* P450 DM) and fluconazole co-crystalline (PDB code: 1EA1) [19] using Molegro Virtual Docker (MVD 2013.6.0.0 [win32]) program [20].

RESULTS

Crystal structure

All bond lengths and angles of the compound **3** structure are within the normal ranges (Table 2). As shown in Figure 1, there are two planes in title molecule which are relevant: isoindol ring C1–C8/N1 form plane I and phenyl ring C16–C21 form plane II. The angle between plane I and II is 79.47 (3)°. The isoindol ring system is planar and piperazine ring (N2/C12/C13/N3/C14/C15) adopts an almost perfect chair conformation. The partial crystal packing diagram of molecule revealed the presence of an intermolecular H-bonding network involving C–H and O functionality with neighboring molecules (Figure 2). The distance of the interactions between H6A...O2 is 2.46 (14) Å and between H20A...O2

Table 2: X-ray and calculated of selected bond lengths (Å) and angles (°) for compound 3

Bond length	Experimental	Calculated (B3LYP/6-31G(d))
O1—C1	1.2020 (18)	1.239
O2—C8	1.2053 (18)	1.239
N1—C1	1.3917 (19)	1.410
N1—C8	1.3942 (19)	1.409
N1—C9	1.456 (2)	1.463
N2—C12	1.456 (2)	1.480
N2—C15	1.456 (2)	1.467
N3—C13	1.456 (2)	1.464
N3—C14	1.454 (2)	1.467
N3—C16	1.403 (18)	1.395
Bond Angles	Experimental	Calculated (B3LYP/6-31G(d))
C1—N1—C8	111.61 (12)	111.94
C1—N1—C9	123.49 (12)	123.98
C8—N1—C9	124.88 (13)	124.06
C11—N2—C12	110.39 (13)	115.97
C11—N2—C15	111.59 (12)	116.32
C12—N2—C15	108.76 (13)	114.87
C13—N3—C14	110.19 (12)	117.03
C13—N3—C16	118.23 (12)	120.85
C14—N3—C16	118.84 (12)	120.03
O1—C1—N1	124.51 (15)	125.06
O1—C1—C2	129.27 (14)	129.14
O2—C8—N1	124.76 (15)	124.99
O2—C8—C7	129.09 (14)	129.20
N1—C8—C7	106.15 (11)	105.79
N1—C9—C10	112.83 (14)	112.73
N2—C11—C10	113.75 (14)	112.32
N2—C12—C13	110.96 (14)	110.22
N3—C13—C12	110.26 (13)	110.37
N3—C14—C15	110.28 (14)	110.97
N2—C15—C14	112.17 (13)	112.84
N3—C16—C17	120.24 (12)	120.85
N3—C16—C21	122.65 (12)	121.56

is 2.52 (9) Å and the angles C6—H6A...O2 is 169.00 (2)° and C20—H20A...O2 is 152.00 (5).

Total energies, frontier molecular orbitals (FMOs) and chemical reactivity

The HOMO and LUMO plots of the title compound are shown in Figure 3. HOMO of the title compound presents a charge density localized mainly on the benzene rings whereas LUMO is centered upon the O—C—N—C—O of the phthalimide moiety. The calculated energy values of HOMO and LUMO are -0.17944 eV and -0.09162 eV, respectively. The HOMO-LUMO energy gap value is 0.08782 eV.

Antibacterial and antifungal activities

The investigation was carried out three times and the average zone of inhibition was calculated. Compound 3 exhibited a good activity against *S. aureus* and *C. albicans* with zones of inhibition of 15 cm and 18 cm, respectively. The remaining strains gave no significant activity with the tested compound.

Molecular docking

In *E. coli* 24 kda domain, clorobiocin (reference compound) was found to have hydrogen bonding

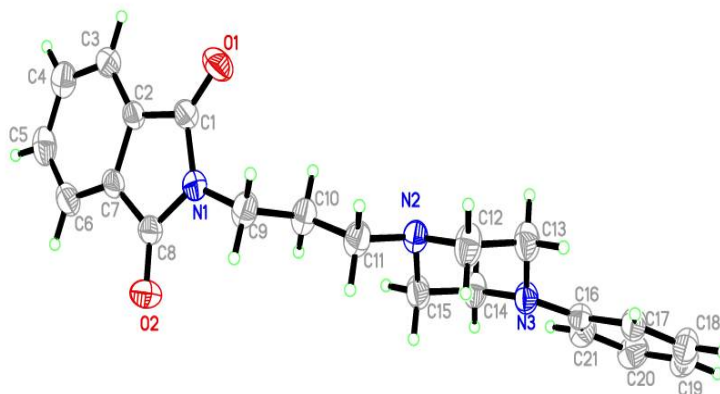


Figure 1: ORTEP diagram of titled compound with thermal ellipsoids at 50 % probability

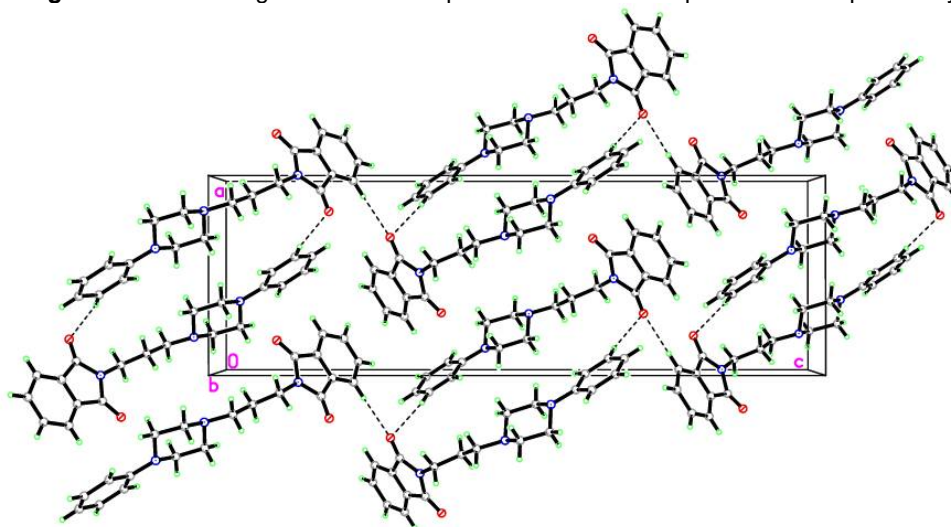


Figure 2: Packing of the molecules in the crystal structure. Dotted lines indicate intermolecular C-H...O interactions

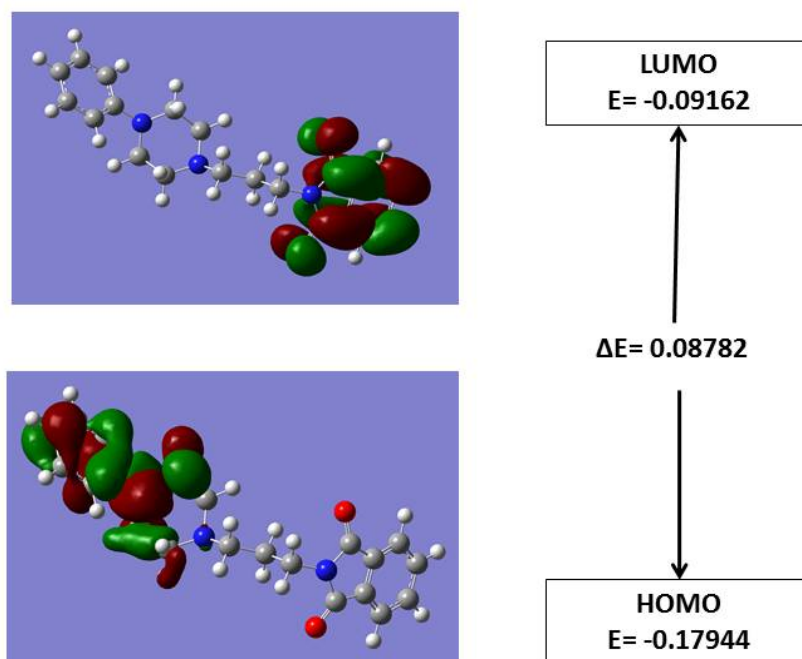


Figure 3: Molecular orbital surfaces and energy levels for the HOMO and LUMO of compound **3** computed at B3LYP/6-31G(d,p) level

interactions with Asn46 (2.76 Å), and Arg136 (2.96, 3.06, 3.44 Å) with MolDock score -175.0 [22]. The compound 3 revealed a MolDock score of -144.29 and form four hydrogen bonding interactions with Asn46 (3.07, 3.39, 3.46 Å) and Gly119 (3.13 Å) (Figure 4a). Figure 4b shows that compound 3 was superimposed with co-crystalline clorobiocin in the active site of the *E. coli* 24 kDa domain.

Regarding the cytochrome P450 14 α -sterol demethylase, the compound 3 revealed a MolDock score -139.15 and form two hydrogen bonding interaction with Arg96 (2.73 Å) and Tyr76 (2.93 Å)(Figure 5a). Figure 5b shows the compound 3 was superimposed with co-crystalline fluconazole in the active site of cytochrome P450 14 α -sterol demethylase and this indicate the good quality of the docking study.

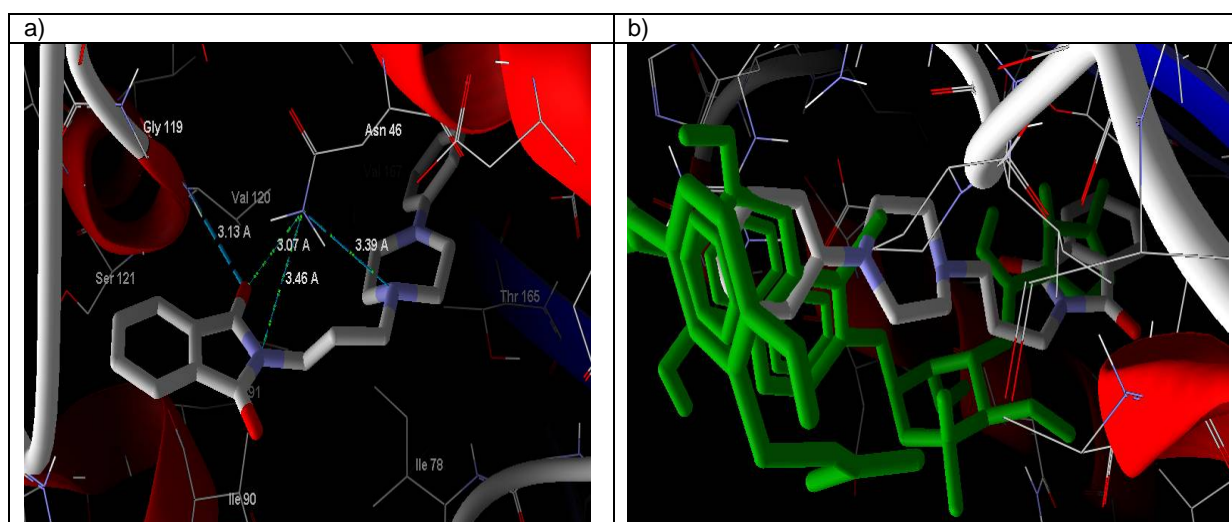


Figure 4: a) Interaction of compound 3 with the active site of the *E. coli* 24 kDa domain; b) Superimpose of the co-crystallized clorobiocin (green) and compound 3 (gray) in the active site of the *E. coli* 24 kDa domain

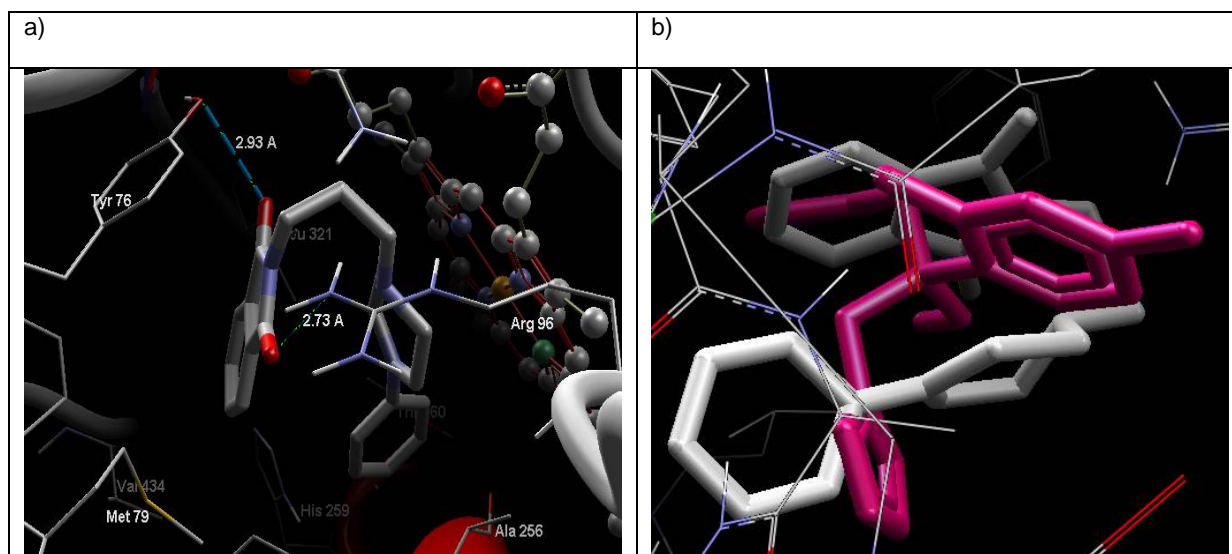


Figure 5: a) Interaction of compound 3 with the active site of cytochrome P450 14 α -sterol demethylase; b) Superimpose of the co-crystallized fluconazole (red) and compound 3 (gray) in the active site of cytochrome P450 14 α -sterol demethylase

DISCUSSION

Most of the optimized bond lengths are slightly higher than the experimental values, due to the molecular states are diverse during the experimental and computed experiments. The theoretical data are calculated in gas phase

without molecular interactions are considered, but the experimental data are collected in the solid state and crystal Interactions, such as Van der Waals forces, hydrogen bond interactions and crystal packing force make slight changes in the structure. Anyway, the computed bond lengths and bond angles are in great

concurrence with the experimental data. Good correlations were obtained between the calculated and experimental bond lengths and angles 0.994 and 0.942, respectively.

HOMO and LUMO are additionally essential in deciding properties, for example, molecular reactivity and the capacity of a molecule to absorb light. To clarify several types of reaction and for foreseeing the most reactive position in conjugated systems, molecular orbitals and their properties like energy are utilized [23]. LUMO (lowest unoccupied molecular orbital) is the molecular orbital of the lowest energy that is not occupied by electrons and speaks the capacity to obtain an electron; HOMO (highest occupied molecular orbital) is molecular orbital of the highest energy that is possessed by electrons and represents the ability to give an electron. The energy gap of HOMO-LUMO clarify the charge exchange inside the molecule and reflect the biological activity of the molecule [24].

The HOMO-LUMO energy gap value is 0.08782 eV. The small energy gaps are generally connected with a high chemical reactivity, low kinetic stability and these molecules are termed as delicate molecules [25].

Compound 3 gives moderate antibacterial and antifungal activities relative to standard drugs, the experimental results have a good agreement with docking results as the compound 3 give MolDock score smaller than the reference drug co-crystallized in the active site of the target enzymes.

CONCLUSION

The title compound, 2-(3-(4-phenylpiperazin-1-yl)propyl)isoindoline-1,3-dione (3) has been synthesized successfully and the optimized molecular structure investigated by B3LYP/6-31G (d,p) method using DFT. HOMO-LUMO energy gap of the molecule is 0.08782 eV. Antimicrobial data show moderate activity against *S. aureus* and *C. albicans*.

ACKNOWLEDGEMENT

The authors would like to extend their sincere appreciation to the Dean of Scientific Research, King Saud University for funding this research through Research Group Project no. PRG-1436-38.

REFERENCES

1. Lobo HR, Singh BS, Shankarling GS. Deep eutectic solvents and glycerol: a simple, environmentally benign and efficient catalyst/reaction media for synthesis of *N*-aryl phthalimide derivatives. *Green Chem Lett Rev.* 2012; 5: 487-533.
2. Han S, Jones RA, Quiclet-Sire B, Zard SZ. A convergent route to functional protected amines, diamines, and β -amino acids. *Tetrahedron.* 2014; 70: 7192-7206.
3. Jarvis CL, Richers MT, Breugst M, Houk K, Seidel D. Redox-Neutral α -Sulfonylation of Secondary Amines: Ring-Fused *N*, *S*-Acetals. *Org Lett.* 2014; 16: 3556-3559.
4. Guo D, Xia L, van Veldhoven JP, Hazeu M, Mocking T, Brussee J, IJzerman AP, and Heitman LH. Binding Kinetics of ZM241385 Derivatives at the Human Adenosine A2A Receptor. *ChemMedChem.* 2014; 9: 752-761.
5. Abdel-Fattah MA, Lehmann J, Abadi AH. An Interactive SAR Approach to Discover Novel Hybrid Thieno Probes as Ligands for D2-Like Receptors with Affinities in the Subnanomolar Range. *Chem Biodivers.* 2013; 10: 2247-2266.
6. Ye N, Song Z, Zhang A. Dual Ligands Targeting Dopamine D2 and Serotonin 5-HT1A Receptors as New Antipsychotical or Anti-Parkinsonian Agents. *Curr Med Chem.* 2014; 21: 437-457.
7. Choi Y-h, Baek DJ, Seo SH, Lee JK, Pae AN, Cho YS and Min SJ. Facile synthesis and biological evaluation of 3, 3-diphenylpropanoyl piperazines as T-type calcium channel blockers. *Bioorg Med Chem Lett.* 2011; 21: 215-219.
8. Bruker. SADABS, APEX2 and SAINT. Bruker AXS Inc., Madison, Wisconsin, USA. 2012.
9. Sheldrick G. SHELXTL, Version 2014/2; Bruker AXS. Inc: Madison, WI. 2014.
10. Spek A. Single-crystal structure validation with the program PLATON. *J Appl Crystallogr.* 2003; 36: 7-13.
11. Macrae CF, Bruno IJ, Chisholm JA, Edgington PR, McCabe P, Pidcock E, Rodriguez-Monge L, Taylor R, Streek Jd, and Wood PA. Mercury CSD 2.0 - new features for the visualization and investigation of crystal structures. *J Appl Crystallogr.* 2008; 41: 466-470.
12. Cheng P-F, Wang C-J, Wang Y-X. 2-(3-Bromopropyl)isoindoline-1, 3-dione. *Acta Crystallogr Sect E Struct Rep Online.* 2009; 65: 2646-2646.
13. Becke AD. Density-functional thermochemistry. III. The role of exact exchange. *J Chem Phys.* 1993; 98: 5648-5652.
14. Ditchfield R, Hehre WJ, Pople JA. Self-consistent molecular-orbital methods. IX. An extended Gaussian-type basis for molecular-orbital studies of organic molecules. *J Chem Phys.* 1971; 54: 724-728.
15. Frisch M, Trucks G, Schlegel H, Scuseria G, Robb M, Cheeseman J, Scalmani G, Barone V, Mennucci B, Petersson GA, Nakatsuji H, Caricato M, Li X, et al.

- Gaussian 09, revision A. 1. Gaussian Inc, Wallingford, CT. 2009.
16. Dennington RD, Keith TA, Millam JM. GaussView 5.0. 8. Gaussian Inc. 2008.
 17. Perez C, Pauli M, Bazerque P. An antibiotic assay by the agar well diffusion method. *Acta Biol Med Exp.* 1990; 15: 113-115.
 18. Lafitte D, Lamour V, Tsvetkov PO, Makarov AA, Klich M, Deprez P, et al. DNA gyrase interaction with coumarin-based inhibitors: the role of the hydroxybenzoate isopentenyl moiety and the 5'-methyl group of the noviose. *Biochemistry.* 2002; 41: 7217-7223.
 19. Podust LM, Poulos TL, Waterman MR. Crystal structure of cytochrome P450 14 α -sterol demethylase (CYP51) from *Mycobacterium tuberculosis* in complex with azole inhibitors. *Proc Natl Acad Sci U S A.* 2001; 98: 3068-3073.
 20. Molegro Virtual Docker (MVD 2013.6.0.0), Molegro bioinformatics solutions, Danish, 2013 <http://www.molegro.com>
 21. Scheldrick G, SADABS B-SADA. Other Correction. Version; 2006.
 22. Thomsen R, Christensen MH. MolDock: a new technique for high-accuracy molecular docking. *J Med Chem.* 2006; 49: 3315-3321.
 23. Choudhary N, Bee S, Gupta A, Tandon P. Comparative vibrational spectroscopic studies, HOMO-LUMO and NBO analysis of N-(phenyl)-2, 2-dichloroacetamide, N-(2-chloro phenyl)-2, 2-dichloroacetamide and N-(4-chloro phenyl)-2, 2-dichloroacetamide based on density functional theory. *Comput Theor Chem.* 2013; 1016: 8-21.
 24. Kavitha E, Sundaraganesan N, Sebastian S. Molecular structure, vibrational spectroscopic and HOMO-LUMO studies of 4-nitroaniline by density functional method. *Indian J Pure Ap Phy.* 2010; 48: 20-30.
 25. Orbitals IFF. Organic Chemical Reactions John Wiley and Sons. New York. 1976.